Provided for non-commercial research and education use.
Not for reproduction, distribution or commercial use.

This article appeared in a journal published by Elsevier. The attached copy is furnished to the author for internal non-commercial research and education use, including for instruction at the authors institution and sharing with colleagues.

Other uses, including reproduction and distribution, or selling or licensing copies, or posting to personal, institutional or third party websites are prohibited.

In most cases authors are permitted to post their version of the article (e.g. in Word or Tex form) to their personal website or institutional repository. Authors requiring further information regarding Elsevier's archiving and manuscript policies are encouraged to visit:

http://www.elsevier.com/copyright

Author's personal copy

Thin Solid Films 520 (2012) 3783–3786

Contents lists available at SciVerse ScienceDirect

Thin Solid Films

journal homepage: www.elsevier.com/locate/tsf

Effect of magnesium oxide passivation on the performance of amorphous indium–gallium–zinc-oxide thin film transistors

Dong Youn Yoo [a,b], Eugene Chong [a,d], Do Hyung Kim [c], Byeong Kwon Ju [b], Sang Yeol Lee [c,*]

[a] Future Convergence Research Division, Korea Institute of Science and Technology, Seoul 136-791, Republic of Korea
[b] Department of Electrical Engineering, Display and Nanosystem Laboratory, Korea University, Seoul, Republic of Korea
[c] Department of Semiconductor Engineering, Cheongju University, Cheongju, Chungbuk, 360-764, Republic of Korea
[d] Nanoelectronics, University of Science and Technology, 113 Gwahangno, Yuseong, Daejeon 305-333, Republic of Korea

ARTICLE INFO

Available online 29 October 2011

Keywords:
MgO
Passivation
Stability
a-IGZO

ABSTRACT

Effect of hygroscopic magnesium oxide (MgO) passivation layer on the stability of amorphous InGaZnO (a-IGZO) thin-film transistors (TFTs) under positive bias stress and positive bias temperature stress has been investigated. The effect of MgO passivation has been observed by comparing the shift of the positive threshold voltage (V_{th}) after constant bias temperature stress, which were 8.2 V for the unpassivated TFTs and 1.88 V for the passivated TFTs.

In addition, MgO passivated a-IGZO TFTs show also excellent stability under a humidity test since MgO passivation layer can prevent the penetration of water into back channel. In order to investigate the origin of humidity test result, we have measured X-ray photoelectron spectroscopy depth profile of both unpassivated and MgO passivated TFTs with a-IGZO back channel layers after N_2 wet annealing.

© 2011 Elsevier B.V. All rights reserved.

1. Introduction

Recently, Zn-based oxide semiconductors are key components in a variety of technologies in flat panel devices. Zn-based oxide thin-film transistors (TFTs) have high mobility, low temperature process, excellent uniformity, and transparency. Amorphous InGaZnO (a-IGZO) TFTs have lots of interest as a strong candidate for next generation devices, such as active-matrix organic light-emitting diodes (AMOLED) and active-matrix liquid crystal display [1–4]. However, the bias-induced instability of TFTs is remained as an issue to be solved, which is a very critical aspect in the adaptation of electric devices for many purposes. The adsorption/desorption of oxygen and water onto the exposed back channel layer causes instability of the threshold voltage in Zn-based oxide TFTs [5–7]. Therefore, passivation layers are necessary for long-term current stability in the operation of the TFTs. So far, various inorganic passivation layers, such as SiO_2, SiN_x, Al_2O_3, TiO_x, and SiON, have been investigated [8,9]. In this paper, we have investigated the effect of MgO passivation on the instability under positive bias temperature stress (PBTS) and positive bias stress (PBS) in a-IGZO TFTs. In addition, we have investigated the effect of water (H_2O) adsorption on the performance of MgO passivated a-IGZO TFTs compared with unpassivated a-IGZO TFTs. It was found that the MgO passivation layer enhanced the stability of a-IGZO TFTs.

2. Experimental procedures

40 nm thick a-IGZO channel layers were deposited on silicon substrate with 200 nm thick SiO_2 as a gate insulator at room temperature by using a radio-frequency (RF) magnetron sputtering method. The deposition was performed at a working pressure of 0.4 Pa and a RF power of 30 W in only Ar (100 sccm) ambient using a 2 inch diameter $InGaZnO_4$ single target (In_2O_3:Ga_2O_3:ZnO = 1:1:2 mol%). The a-IGZO channel layers were patterned by wet-etching. The Au (55 nm)/Ti (15 nm) electrodes for source and drain were fabricated using an e-beam evaporator and conventional photolithography with lift-off process. The channel width and length of the TFT devices were 250 and 50 μm, respectively. All of the fabricated TFT devices were heat treated in a furnace at 350 °C with a nitrogen atmosphere for 2 h. Finally, the passivation layers were deposited by pulsed laser deposition method at a process pressure of 350 mTorr and a pulsed laser power density of 1.2 J/cm^2 at room temperature in an O_2 (oxygen content is 50 sccm) ambient using a 2 inch diameter MgO and SiO_2 single target. 9 devices were fabricated on one substrate (11 × 11 mm^2) at the same time in order to compare the reproducibility of BTS, and these devices have shown similar performance in each condition. For the humidity experiments, the TFTs were dipped in distilled water and out to be measured. Then, the electrical properties of the devices were measured at room temperature in dark box by semiconductor parameter analyzer (ELECS-EL423). In addition, to investigate the origin of humidity test result, we have measured X-ray photoelectron spectroscopy (XPS) depth profile of a-IGZO back

* Corresponding author. Tel.: +82 43 229 8534; fax: +82 43 229 8110.
E-mail address: sylee@cju.ac.kr (S.Y. Lee).

0040-6090/$ – see front matter © 2011 Elsevier B.V. All rights reserved.
doi:10.1016/j.tsf.2011.10.065

Author's personal copy

channel layers of unpassivated, SiO_2, and MgO passivated devices after N_2 wet annealing.

3. Results and discussions

The results of the field effect mobility (μ_{FE}), threshold voltage (V_{th}), on–off current ratio ($I_{on/off}$), and subthreshold swing (S.S) for unpassivated, SiO_2, and MgO passivated a-IGZO TFTs are listed in Table 1. The μ_{FE} at a drain voltage (V_{DS}) of 10.1 V is calculated by $\mu_{FE} = I_{DS} \cdot 2L/(C_i \cdot W)(V_{GS} - V_{th})^2$ in the saturation regime, where C_i, V_{th}, W and L denote the gate capacitance, threshold gate voltage, channel width and length, respectively [9,10]. The V_{th} was determined by adjusting the gate voltage (V_{GS}), which induces a drain current of L/W × 10 nA at V_{DS} = 10.1 V. In addition, the S.S was extracted from the linear portion of the log(I_{DS})-versus-V_{GS} plot by using [11];

$$S.S = \left(\frac{d \log I_{DS}}{dV_{GS}}\right)^{-1} \quad (1)$$

It is interesting to note that the shift in V_{th} of TFT with MgO passivation under PBTS was reduced than those of SiO_2 passivated and unpassivated TFTs as shown in Fig. 1. Fig. 1 shows the evolution of the transfer curve as a function of the applied PBTS time for unpassivated, SiO_2, and MgO passivated TFTs. The TFTs were stressed under the following conditions; we have applied V_{GS} = 10.1 V and V_{DS} = 10.1 V to measure transfer curve for PBTS test. V_{GS} values at I_{DS} of 10 μA at 60 °C of unpassivated, SiO_2, and MgO passivated devices have been set at 16.8 V, 16 V, and 15.5 V for PBTS test, respectively. After that the transfer curves of three devices have been measured at a bias stress of V_{GS} = 10.1 V and V_{DS} = 10.1 V. The maximum stress duration was 420 min [12]. Considering that a I_{DS} of approximately 3 μA is required to manifest the full white color of 300 nit in the AMOLED device [13], the applied stress current (10 μA) corresponds to very severe test conditions. The V_{th} of the SiO_2 and MgO passivated a-IGZO TFTs shifted by +2.1 V and +1.88 V, respectively, after 420 min of PBTS as shown in Fig. 1. However, the V_{th} of the unpassivated a-IGZO TFT shifted as much as +8.2 V. These results demonstrate that the MgO passivated a-IGZO TFTs are effective in the stability improvement of the a-IGZO TFTs. Other parameters, such as μ_{FE} and S.S, do not change much during the PBTS test. The positive V_{th} shift in Zn-based oxide TFTs under PBTS has been explained by charge trapping or defect creation [14,15]. However, the positive shift in V_{th} without significant change in the μ_{FE} and S.S during stress time is not attributed to defect creation within the channel layer. The difference in the instability of V_{th} among the devices is caused mainly by the difference in the gate voltage initially applied to induce the 10 μA drain current because relatively large vertical electrical field for unpassivated device causes more charge trapping [16].

We also investigated the effects of PBS. The positive shift in threshold voltage can be explained using a charge trapping model [17]. Fig. 2 shows the effect of the PBS on devices. The conditions for PBS were V_{GS} = 15 V and V_{DS} = 0 V for 120 min. Unpassivated, SiO_2, and MgO passivated a-IGZO TFTs have same gate dielectric and active layer. So, the charge trapping at the channel/dielectric interface during gate voltage stress would be predicted to be similar with each other [18]. However, the V_{th} shifts for unpassivated, SiO_2, and MgO passivated a-IGZO

Table 1
Comparison of the measured electrical parameters for unpassivated and SiO_2, and MgO passivated TFTs. (V_{GS} values of unpassivated, SiO_2, and MgO passivated devices have been set at 16.8 V, 16 V, and 15.5 V, respectively, at I_{DS} of 10 μA at 60 °C for PBTS test).

	V_{th} (V)	μ_{FE} (cm^2/V·s)	S.S (V/decade)
Unpassivation	7.50	4.53	0.12
420 min (PBTS test)	15.70	4.94	0.10
SiO_2 passivation	5.10	4.42	0.12
420 min (PBTS test)	7.2	4.71	0.11
MgO passivation	4.50	3.98	0.09
420 min (PBTS test)	6.38	4.18	0.08

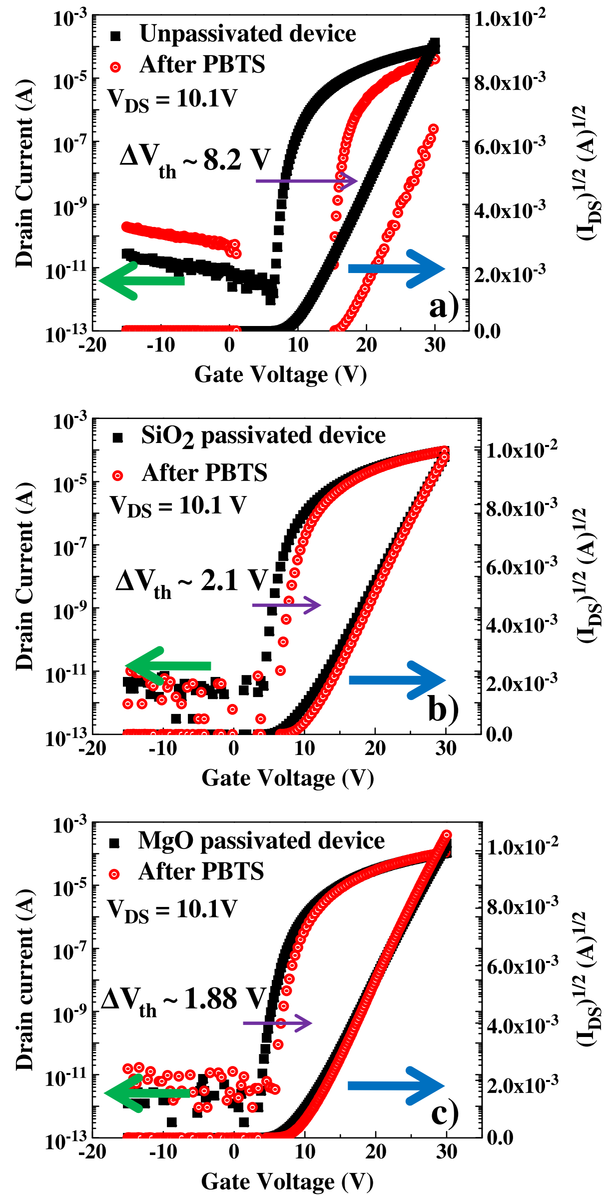

Fig. 1. Time evolution of V_{th} during PBTS of (a) unpassivated, (b) SiO_2 passivated, and (c) MgO passivated a-IGZO TFTs.

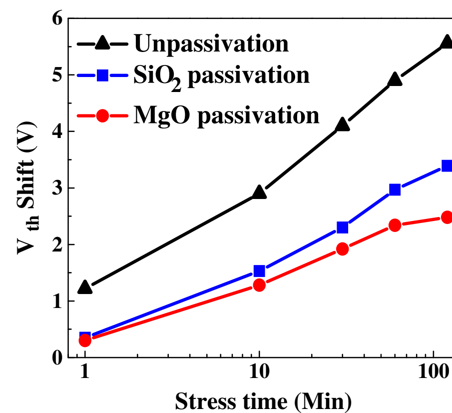

Fig. 2. Dependence of the V_{th} shift on the gate bias stresses for unpassivated, SiO_2, and MgO passivated devices.

Author's personal copy

TFTs were 5.56, 3.39, and 2.48 V, respectively. In the beginning, we thought charge trapping can explain the positive threshold voltage shift. But, because of positive shift difference in threshold voltage of devices, we found that charge trapping model was not enough to explain the results obtained. And we suggest that the adsorption/desorption of oxygen and water onto the exposed back channel layer plays a critical role in determining the instability of the threshold voltage in oxide TFTs. In order to obtain the information on the H_2O-related behavior, the performance of unpassivated, SiO_2, and MgO passivated a-IGZO TFTs on the change of V_{th}, S.S and $I_{on/off}$ has been investigated in detail. Fig. 3 shows the cross section diagram of a MgO passivated a-IGZO TFTs exposed to water. The devices were dipped and kept in distilled water overnight (12 h), and then they were naturally dried at room temperature for 21 h and 25 min in dark box in air. The transfer curves before and after the exposure to the humidity conditions mentioned above were compared. Fig. 4(a), (b), and (c) shows transfer curves obtained with the unpassivated, 20-nm-thick SiO_2, and MgO passivated a-IGZ TFTs, respectively. The interfacial trap density (N_{it}) can be obtained by solving the following equation;

$$N_{it} = \left[\frac{S.S\log(e)}{kT/q} - 1\right]\frac{C_i}{q} \quad (2)$$

where q is the elementary electron charge, T is the absolute temperature, k is Boltzmann constant, and C_i is the gate capacitance per unit area [19–21]. It was important to note that the parameters, such as V_{th}, $I_{on/off}$, and S.S, were hardly changed for SiO_2 and MgO passivated a-IGZO TFTs while the electrical performance was degraded due to H_2O adsorption on a-IGZO surface for unpassivated a-IGZO TFTs same as reported by Park et al. [22]. In the case of unpassivated TFTs, the interfacial trap densities were changed from $2.63\times10^{11}\,cm^2$ to $4.33\times10^{12}\,cm^2$. On the contrary, the interfacial trap densities were hardly changed from $9.63\times10^{10}\,cm^2$ to $2.26\times10^{11}\,cm^2$ and from $5.92\times10^{10}\,cm^2$ to $9.63\times10^{10}\,cm^2$ in the case of SiO_2 and MgO passivated TFTs, respectively.

For additional humidity test, we investigated wet annealing process with unpassivated, SiO_2 and MgO passivated a-IGZO TFTs under the following conditions; the devices were subjected to thermal annealing at 200 °C for 2 h in a wet N_2 atmosphere. After wet annealing, the chemical and structural evolution of a-IGZO films with unpassivated, SiO_2, and MgO passivated TFTs were analyzed by XPS. Fig. 5(a), (b), and (c) represents the de-convolution of O 1s peak of XPS spectra by the method of curve fitting for IGZO films. Since the etching rate by sputter of XPS is about 4 nm/0.1 min for a-IGZO thin films, the sputtering time can be considered as depth profile of a-IGZO channel layer. In addition, channel layer thickness of three devices is same as 40 nm. However, passivation layer thickness is 20 nm. In order to investigate the depth profile of same point of channels of three devices depending on wet annealing process, we analyzed XPS spectrum at 0.1, 0.6, and 0.6 min as a function of sputtered time which means O 1s peak of surface of a-IGZO channel in the case of unpassivated, SiO_2 and MgO passivated, respectively. The

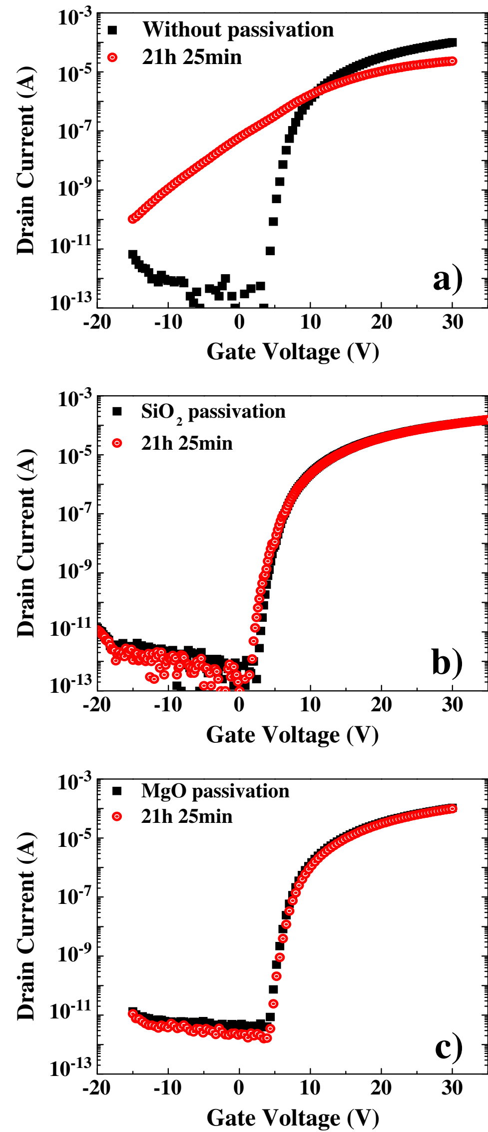

Fig. 4. The transfer curves of (a) unpassivated a-IGZO TFTs, (b) 20-nm-thick SiO_2 passivated a-IGZO TFTs, and (c) 20-nm-thick MgO passivated a-IGZO TFTs. The devices were dipped and kept in distilled water overnight (12 h) and then they were dried at room temperature for 21 h and 25 min in a dark box.

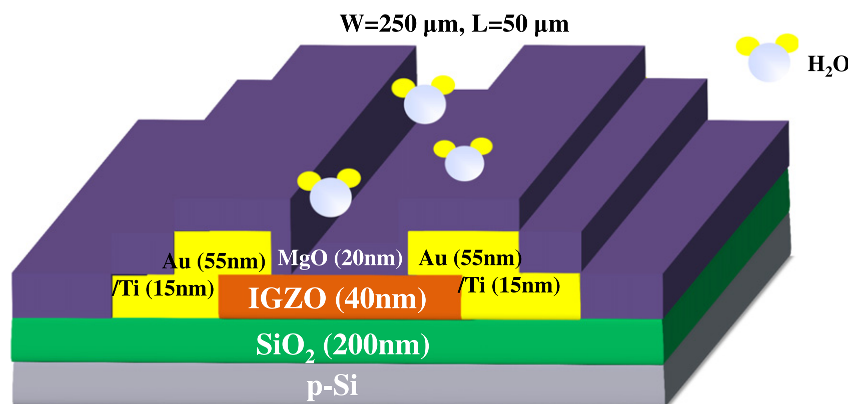

Fig. 3. The schematic diagram of MgO passivated a-IGZO TFTs exposed to water. The magnesium hydroxide forms in the presence of water ($MgO + H_2O \rightarrow Mg(OH)_2$).

Author's personal copy

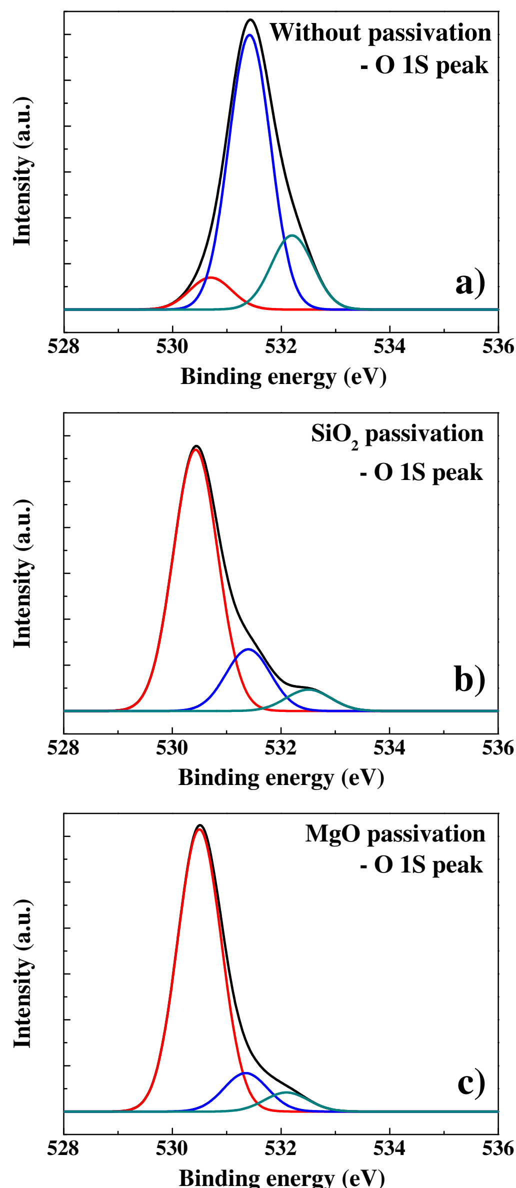

Fig. 5. O 1s peak de-convolution of XPS spectra for a-IGZO back channels with (a) unpassivated, (b) SiO_2, and (c) MgO passivated TFTs.

O 1s peaks centered at binding energies of 530.5 eV, 531.5 eV, and 532.5 eV are related with oxygen in oxide lattices without oxygen vacancies, with oxygen vacancies, and with OH^- impurities, respectively [23]. It can be clearly observed that the relative area of the oxygen vacancy-related peak decreased with unpassivated and passivated layers. The values are 75.88%, 17.90%, and 11.31% for unpassivated, SiO_2, and MgO passivated TFTs, respectively. Therefore, the MgO passivation layer can easily react with absorbed water molecules to form magnesium hydroxides due to its hygroscopic properties [24]. As a suspension in water, magnesium hydroxide has low solubility [25]. So, the magnesium hydroxide layer on MgO passivation layer can prevent the penetration of water into back channel [26,27].

4. Conclusions

In conclusion, the electrical performance of a-$InGaZnO_4$ TFTs fabricated on SiO_2/Si substrates has been investigated. Especially, the performance of unpassivated, SiO_2, and MgO passivated TFTs was compared in this work. The MgO passivation layer could significantly reduce the change in the threshold voltage and subthreshold gate-voltage swing under PBTS and PBS compared with those of unpassivated devices. In addition, we investigated the effect of the humidity on a-IGZO TFTs with MgO passivation. As a result, the effect of the adsorption/desorption of oxygen and water onto the exposed back channel layer, which causes the threshold voltage shift in oxide TFTs, is significantly reduced due to hygroscopic nature of MgO passivation layer. Therefore, it is important to adopt MgO passivation layer to improve the device long term bias-stress stability for the wide range of possible applications.

References

[1] K. Nomura, H. Ohta, A. Takagi, T. Kamiya, M. Hirano, H. Hosono, Nature (London) 432 (2004) 488.
[2] K. Nomura, H. Ohta, K. Ueda, T. Kamiya, M. Hirano, H. Hosono, Science 300 (2003) 1269.
[3] J.S. Park, K.S. Kim, Y.G. Park, Y.G. Mo, H.D. Kim, J.K. Jeong, Adv. Mater. 21 (2009) 329.
[4] D. Kim, Y. Choi, H.L. Tuller, Appl. Phys. Lett. 87 (2005) 043509.
[5] H.K. Kim, K.S. Lee, J.H. Kwon, Appl. Phys. Lett. 88 (2006) 012103.
[6] M. Kim, J.H. Jeong, H.J. Lee, T.K. Ahn, H.S. Shin, J.-S. Park, J.K. Jeong, Y.-G. Mo, H.D. Kim, Appl. Phys. Lett. 90 (2007) 212114.
[7] E.M.C. Fortunato, P.M.C. Barquinha, A.C.M.B.G. Pimentel, A.M.F. Goncalves, A.J.S. Marques, L.M.N. Pereira, R.F.P. Martins, Adv. Mater. 17 (2005) 590.
[8] W. Lim, E.A. Douglas, D.P. Norton, S.J. Peartona, F. Ren, Y.-W. Heo, S.Y. Son, J.H. Yuh, J. Vac. Sci. Technol. B 28 (2010) 1.
[9] C.R. Kagan, P. Andry, Thin-Film Transistors, M. Dekker, New York, 2003, p. 85, Chapter 3.
[10] E.M.C. Fortunato, P.M.C. Barquinha, A.C.M.B.G. Pimentel, A.M.F. Gonçalves, A.J.S. Marques, R.F.P. Martins, L.M.N. Pereira, Appl. Phys. Lett. 85 (2004) 2541.
[11] Y. Vygranenko, K. Wang, A. Nathan, Appl. Phys. Lett. 91 (2007) 263508.
[12] H.S. Seo, J.U. Bae, D.H. Kim, Y.J. Park, C.D. Kim, I.B. Kang, I.J. Chung, J.H. Choi, J.M. Myoung, Electrochem. Solid-State Lett. 12 (2009) H348.
[13] H.S. Seo, D.H. Nam, N.B. Choi, S.H. Paek, T.J. Ahn, J.S. Yoo, S.W. Lee, C.D. Kim, I.J. Chung, IDW Proceeding, ITE and SID, 2005, p. 1129.
[14] R.B.M. Cross, M.M. De Souza, Appl. Phys. Lett. 89 (2006) 263513.
[15] P. Gorrn, P. Holzer, T. Riedl, W. Kowalsky, J. Wang, T. Weimann, P. Hinze, S. Kipp, Appl. Phys. Lett. 90 (2007) 063502.
[16] J. Yuan, J. Zhang, J. Wang, D. Yan, W. Xu, Thin Solid Films 450 (2004) 316.
[17] A. Suresh, J.F. Muth, Appl. Phys. Lett. 92 (2008) 033502.
[18] J.K. Jeong, H.W. Yang, J.H. Jeong, Y.-G. Mo, H.D. Kim, Appl. Phys. Lett. 93 (2008) 123508.
[19] E. Chong, Y.S. Chun, S.Y. Lee, Electrochem. Solid-State Lett. 14 (2011) H96.
[20] J.K. Jeong, S. Yang, D.-H. Cho, S.-H.K. Park, C.-S. Hwang, K.I. Cho, Appl. Phys. Lett. 95 (2009) 123505.
[21] Y. Kagan, P.W.E. Andry, Thin Film Transistors, Dekker, New York, 2003, p. 87, Chap. 3.
[22] J.S. Park, J.K. Jeong, H.-J. Chung, Y.-G. Mo, H.D. Kim, Appl. Phys. Lett. 92 (2008) 072104.
[23] G.H. Kim, W.H. Jeong, H.J. Kim, Phys. Status Solid A. 207 (2010) 1677.
[24] H.S. Jung, J.K. Lee, K.S. Hong, H.J. Youn, J. Appl. Phys. 92 (2002) 2855.
[25] H.S. Jung, J.-K. Lee, M. Nastasi, Appl. Phys. Lett. 88 (2006) 013107.
[26] O.E. Taurian, M. Springborga, N.E. Christensen, Solid-State Commun. 55 (1985) 351.
[27] Jimmy C. Yu, Xu. Anwu, Lizhi Zhang, Ruiqi Song, Wu. Ling, J. Phys. Chem. B. 108 (2004) 64.